Stability Prediction in Tiltrotor Aircraft Including Rotor-Wing Aerodynamic Interaction

Taeseong Kim,[1]
[1]*School of Mechanical and Aerospace Engineering*
Building 301 Room 1313, Seoul National University, 56-1, Shillim-Dong, Kwanak-Gu, Seoul,151-744, Korea
Tel : +82-2-880-1901, Fax : 82-2-887-2662, e-mail: kimts77@snu.ac.kr

SangJoon Shin,[2]
[2]*Seoul National University, School of Mechanical and Aerospace Engineering, Institute of Advanced Aerospace Technology, Room 1418 Building 301, San 56-1, Sillim-Dong, Gwanak-Gu, Seoul, 151-744, Korea.*
Tel : +82-2-880-1642, Fax : 82-2-887-2662, e-mail: ssjoon@snu.ac.kr

and Do-Hyung Kim[3]
[3] *Korea Aerospace Research Institute, Rotor Department, 45 Eoeun-Dong, Yuseong-Gu, Daejeon, 305-333, Korea.*
e-mail: dhkim@kari.re.kr

Key words: Whirl flutter, unsteady aerodynamics, aerodynamic interaction, tiltrotor aircraft

ABSRACT

Aeroelastic stability analysis is conducted regarding a tiltrotor aircraft with several aerodynamic models in time and frequency domain. Two significant structural features, which are the control system flexibility and wing sweep, are considered. Three different aerodynamic models, a normal, Greenberg's quasi-steady, and full unsteady aerodynamic model, are used for the rotor. The two-dimensional strip theory is adopted for the wing. The influence of torsion and bending coupling effect gives a lowered flutter speed. The wing aerodynamic force increases it due to aerodynamic damping. Two different quasi-steady aerodynamic models show the similar stability boundary. The unsteady aerodynamics is also adopted and compared with the previous results by quasi-steady aerodynamics. The highest flutter boundary is obtained by the full unsteady aerodynamics.

1. INTRODUCTION

The whirl flutter instability, which is induced by the inplane hub forces, generally imposes a limit on the cruise performance in tiltrotor aircraft. Therefore, precise estimation of the whirl flutter instability is required to enhance cruise performance of the aircraft. Many researches have been conducted to estimate and improve aeroelastic stability boundary using several design parameters and control methods [1-9]. However it is recognized that those investigations have not considered an important phenomenon, which is an unsteady aerodynamic environment which occurs near the rotor and wing. The unsteady aerodynamic formulation needs to be included to represent realistic aerodynamic environment existing in a tiltrotor aircraft. By including unsteady aerodynamic effect, it is possible to establish a complete analytical model which is capable of more precise prediction for a tiltrotor aircraft than the previous models were capable of.

The analytical modeling procedure is also important for a more accurate result since a tiltrotor aircraft consists of more complicated structural mechanism than the other rotorcraft does. It consists of large diameter flapping rotors, which are mounted at the wing tip. The wing motions are dominated by the rotor hub forces and moments. The rotor hub forces and moments are transmitted to the wing tip through the mast. The wing motions, which are elastic bending and torsion, are also transmitted to the rotor shaft. Therefore an accurate structural modeling procedure is essentially

required for a precise analysis. In this paper, the wing sweep is considered to include wing elastic coupling between torsion and bending.

Aerodynamic interaction between the rotor and wing is another factor which may influence to a significant extent on the whirl flutter stability in a tiltrotor aircraft. Such interaction has been included in the investigation originally due to that it was an additional complicacy in tiltrotor aerodynamics [10-14]. Throughout those studies, it was found that the wake developed from the rotor blades influences upon the wing, such as vibration induced at the wing and fuselage. Such induced vibration is expected to affect the whirl flutter stability of the aircraft.

In this paper, an analytical framework is developed with an unsteady aerodynamic model for a more precise whirl flutter prediction. A complete tiltrotor aircraft, which includes a flexible wing with a sweep, control system flexibility, and a gimballed hub, is formulated to investigate the whirl flutter stability.

2. ANALYTICAL MODEL

2.1 Structural and Aerodynamic Modeling

The present structural model is shown in Fig. 1. The total nine degrees of freedom, which consist of three rotor blade flapping (β_0, β_{1C} and β_{1S}), lead-lag (ς_0, ς_{1C} and ς_{1S}) motions of the the rotor, and three elastic wing (q_1, q_2 and p) motions, are utilized. It is explained in detail in the Ref. 15. Control system flexibility is also considered with the pitch-flap ($K_{p\beta}$) and pitch-lag ($K_{p\varsigma}$) coupling parameters. Using the effective parameters with respect to the aircraft flight speed control system flexibility can be included [6, 15].

The rotor and wing motions are coupled. The dynamic motions are transmitted through the shaft at the wing tip. The wing sweep is considered, and therefore the wing tip displacement and rotations are decomposed with torsion and bending coupled motion. For example, vertical bending motion is produced by vertical displacement and shaft roll motion for the unswept wing, but on the other hand, shaft pitch motion is added to produce the vertical bending motion for the swept wing. The detail expression is presented in Ref. 4.

The aerodynamic formulation is obtained with an assumption that the tiltrotor aircraft is in a purely axial flow in equilibrium. Only a perturbation component in aerodynamics is considered in this paper. Trim state is assumed to be established already and the perturbation from it is considered for flutter analysis. In this paper, three different aerodynamic models on the rotor are used to predict whirl flutter stability in frequency domains. Time domain analysis is conducted using the simplest aerodynamic model. The first aerodynamic model is widely used and is quoted as a normal quasi-steady aerodynamics in this paper. This aerodynamic model is developed based on Ref. 4. The second quasi-steady aerodynamic model is cited as Greenberg's quasi-steady aerodynamic model in this paper whose detailed equation is described in Eq. (2). It is equivalent to replacing $C(k)$ by unity in Greenberg's aerodynamic model [16, 17]. For a full unsteady aerodynamic representation, Greenberg's two-dimensional unsteady aerodynamic model is used [17]. Its expression is also presented in Eq. (3). Both in Greenberg's quasi-steady and in full unsteady aerodynamic model, noncirculatory terms are ignored. Since a thin airfoil theory is adapted in the present derivation, the effects of noncirculatory terms are very small compared with the circulatory ones [18]. The two dimensional strip theory is also used on the wing because generally the considered wing for the tiltrotor aircraft is assumed to have high aspect ratio.

$$L = 2\pi\rho U(t)^2 b\alpha(t) \tag{1}$$

$$L = \underbrace{2\pi\rho U(t)b[(\dot{h}(t)+U(t)\theta(t))+b(\frac{1}{2}-a_h)\dot{\theta}(t)_{ref}]}_{Circulatory\ part(L_C)} + \underbrace{\pi\rho b^2[(\dot{h}(t)+U(t)\theta(t)\dot{)}-ba_h\ddot{\theta}(t)_{ref}]}_{Noncirculatory\ part(L_{NC})} \quad (2)$$

$$L = \underbrace{2\pi\rho U(t)bC(k)[(\dot{h}(t)+U(t)\theta(t))+b(\frac{1}{2}-a_h)\dot{\theta}(t)_{ref}]}_{Circulatory\ part(L_C)} + \underbrace{\pi\rho b^2[(\dot{h}(t)+U(t)\theta(t)\dot{)}-ba_h\ddot{\theta}(t)_{ref}]}_{Noncirculatory\ part(L_{NC})} \quad (3)$$

where $\dot{h}(t) = -\delta u_p(t)cos\phi + \delta u_T(t)sin\phi$.

The final form of the structural equation is arranged in the left hand side (LHS) in governing equations, while the aerodynamic equation is in the right hand side (RHS) of the same equation. More detail expressions of equation are described in Ref. 19.

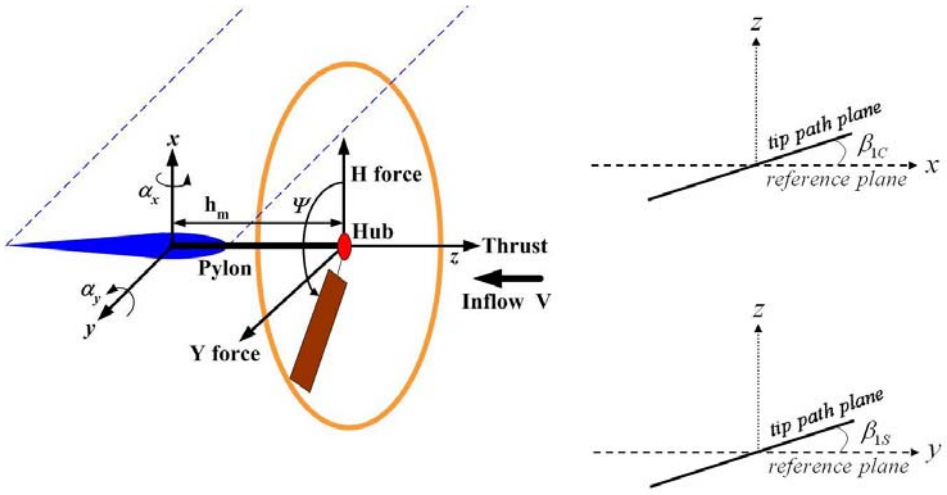

Figure 1. Rotor system with a completely rigid blade

2.2 Aeroelastic Stability Analysis

After combining structural and aerodynamic part, two different types of governing equations, which correspond to quasi-steady and full unsteady aerodynamic model, are obtained. First, the governing equations for the normal and Greenberg's quasi-steady aerodynamic model can be written as follows.

$$M_s\ddot{y} + C_s\dot{y} + K_s y = C_a\dot{y} + K_a y + G_a p + Z_a g \quad (4)$$

where $y^T = \{\beta_{1C} \quad \beta_{1S} \quad \varsigma_{1C} \quad \varsigma_{1S} \quad \beta_0 \quad \varsigma_0 \quad q_1 \quad q_2 \quad p\}$, $p^T = \{\theta_{1C} \quad \theta_{1S} \quad \theta_0\}$,

$g^T = \{u_G \quad \beta_G \quad \alpha_G\}$, and the subscript *a* and *s* mean an aerodynamic part and a structural part, respectively. All elements of the matrices are dimensionless.

Converting Eq. (4) into a state space form gives

$$\dot{Y} = \underbrace{\begin{bmatrix} 0 & I \\ -B & -A \end{bmatrix}}_{18\times18} \underbrace{\begin{Bmatrix} y \\ \dot{y} \end{Bmatrix}}_{18\times1} + \underbrace{\begin{bmatrix} 0 & 0 \\ \bar{G} & \bar{Z} \end{bmatrix}}_{18\times6} \underbrace{\begin{Bmatrix} p \\ g \end{Bmatrix}}_{6\times1} \tag{5}$$

where $\bar{C} = (C_s - C_a)$, $\bar{K} = (K_s - K_a)$, $A = (M_s^{-1}\bar{C})$, $B = (M_s^{-1}\bar{K})$, $\bar{G} = (M_s^{-1}G_a)$

$\bar{Z} = (M_s^{-1}Z_a)$ and $Y^T \equiv \{y \quad \dot{y}\}$.

Second, the governing equation for the full unsteady aerodynamic model is slightly different with quasi-steady aerodynamic one because of the lift deficiency function, $C(k)$, which is formulated only in frequency domain. Therefore Jones' approximation is utilized to predict the stability boundary in time domain [20, 21]. Then the new quantities, the augmented state variables, are obtained. The resulting augmented state variables are associated with a downwash velocity at the three quarter chord location [22]. They describe the unsteady effects. In this paper, the augmented state variables of the typical section at $3/4$ span location are utilized as an averaged value.

After adopting Jones' approximation, the governing equation will be in a form of the state space equations as follows.

$$\begin{bmatrix} \dot{Y} \\ \dot{X} \end{bmatrix} = \underbrace{\begin{bmatrix} \underbrace{T^*}_{18\times18} & \underbrace{S^*}_{18\times4} \\ \underbrace{D}_{4\times18} & \underbrace{E}_{4\times4} \end{bmatrix}}_{22\times22} \underbrace{\begin{bmatrix} Y \\ X \end{bmatrix}}_{22\times1} + \underbrace{\begin{bmatrix} \underbrace{O^*}_{18\times6} \\ \underbrace{0}_{4\times6} \end{bmatrix}}_{22\times6} \underbrace{\begin{bmatrix} p \\ g \end{bmatrix}}_{6\times1} \tag{6}$$

where $T^* = \underbrace{\begin{bmatrix} 0 & I \\ -B & -A \end{bmatrix}}_{18\times18}$, $S^* = \underbrace{\begin{Bmatrix} 0 \\ C \end{Bmatrix}}_{18\times4}$, $\mathrm{O}^* = \underbrace{\begin{bmatrix} 0 & 0 \\ \bar{G} & \bar{Z} \end{bmatrix}}_{18\times6}$, $E = \begin{bmatrix} a_{11} & a_{12} \\ 1 & 0 \end{bmatrix}$, $D = \begin{Bmatrix} 1 \\ 0 \end{Bmatrix}$, $v = \underbrace{\begin{Bmatrix} p \\ g \end{Bmatrix}}_{6\times1}$,

$A = (\bar{M}^{-1}\bar{C})$, $B = (\bar{M}^{-1}\bar{K})$, $C = (\bar{M}^{-1}Z_a)$, $\bar{M} = (M_s - M_a)$, $\bar{C} = (C_s - C_a)$, $\bar{K} = (K_s - K_a)$,
$\bar{G} = (M_s^{-1}G_a)$, and $\bar{Z} = (M_s^{-1}Z_a)$.

3. NUMERICAL RESULTS

Numerical investigation is conducted to obtain the aeroelastic stability boundary with the three different aerodynamic models. An autorotation condition is considered as a rotor operating condition. Since the perturbations in the control pitch input and gust are not considered in the present analysis, $\bar{G}$, $\bar{Z}$, and O^* matrices may be ignored in Eqs. (5) and (6). The numerical values of the structural parameters are based on Ref. 4. An influence of wing sweep on the aircraft stability is investigated, and in which damping ratio is evaluated in terms of the wing vertical bending mode (q_1) with and without sweep.

3.1 Effects of Coupled Bending and Torsion Modes

The coupled bending and torsion modes can be considered by the wing sweep. The effect of the coupled bending and torsion modes is quite substantial. One of the most important features of the swept wing is that the location of the wing tip elastic axis is changed and therefore the distance from the effective elastic axis to the rotor hub is varied. The forward sweep, -6.5°, is considered in the present analysis. Figure 2 shows q_1 mode behaviors in terms of the wing sweep. The present coupled mode analysis with the wing sweep results in a decreased stability boundary. The swept wing stability boundary becomes approximately 120 *knots* lower than that for the straight wing. It is concluded that the sweep may influence the aeroelastic stability. Therefore all the foregoing results are based on the swept wing configuration. A similar trend is observed in Refs. 4 and 5.

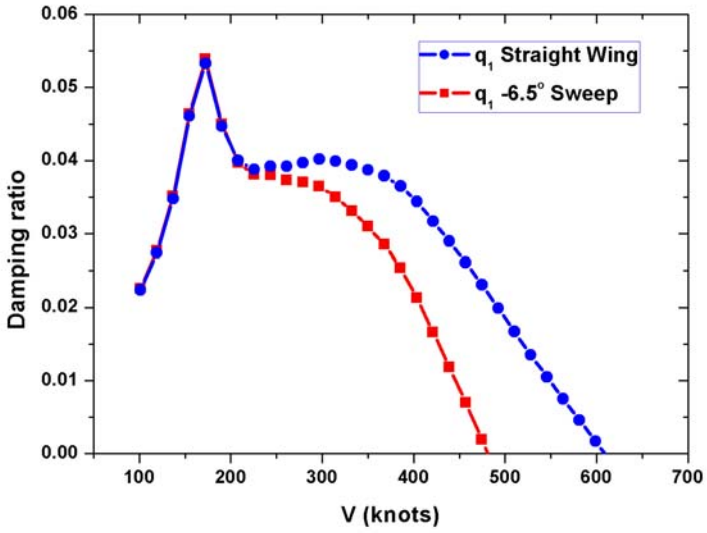

Figure 2 : Damping ratio of the wing vertical bending mode with respect to sweep

3.2 Effect of the Wing Aerodynamics

Influence of the wing aerodynamics is analyzed with regard to the stability boundary with and without wing aerodynamics. Figure 3 shows the damping results of the wing vertical bending (q_1) mode. The basic model includes the wing aerodynamics while the simplified model does not contain it. The wing sweep is considered in both models. The basic model becomes unstable later

the than simplified one does because of the aerodynamic damping effect. There is approximately 70 *knots* difference between each other.

Generally, the vertical wing mode becomes unstable first among the nine degrees of freedom considered. Therefore only the wing degree of freedom should be illustrated in the following.

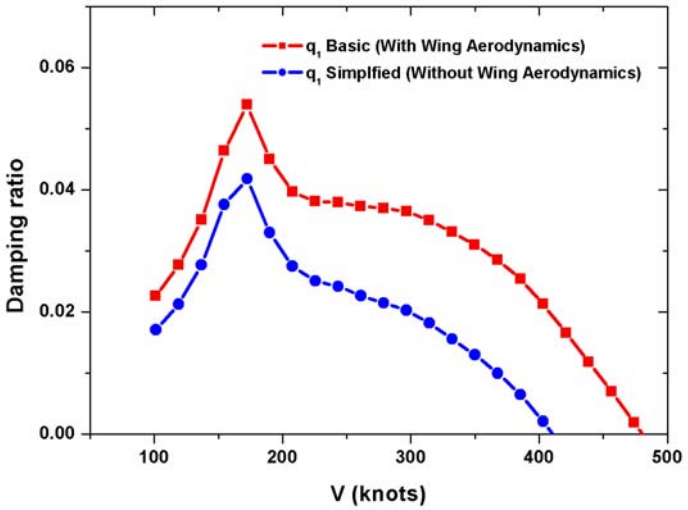

Figure 3 : Comparison results regarding the wing aerodynamics

3.3 Effect of the Control System Flexibility

The control system flexibility is considered using pitch-flap and pitch-lag coupling parameters. The rotor blade has a net flap and lag moment in cruise flight condition because of aerodynamic and centrifugal forces when the blade lags and flaps, respectively. The principal effects of those moments are to produce a static pitch deflection due to the control system flexibility. The effective pitch-flap and pitch-lag couplings are introduced by those effects. The considered couplings are represented as follows. [23]

$$K_{P_\beta} = -\frac{\partial\theta}{\partial\beta} = \frac{1}{K_\theta}\left[I_b(\nu_\beta{}^2 - 1 - \nu_\varsigma{}^2)\varsigma + K_\varsigma \varsigma_P \right]$$
$$K_{P_\varsigma} = -\frac{\partial\theta}{\partial\varsigma} = \frac{1}{K_\theta}\left[I_b(\nu_\beta{}^2 - 1 - \nu_\varsigma{}^2)\beta - K_\beta \beta_P \right] \quad (7)$$

where K_θ, K_β, K_ς, β_P and ς_P represent control system flexibility, flap hinge spring constant, lag hinge spring constant, precone angle, and prelag angle, respectively.

If the stiff control system is considered then K_θ term goes to infinite. It means that pitch-flap and pitch-lag couplings are zero values. In order words, using effective pitch-flap and pitch-lag coupling by collective pitch angle the control system flexibility may be utilized. Figure 4 shows the variation of those coupling parameters for the considered aircraft model.

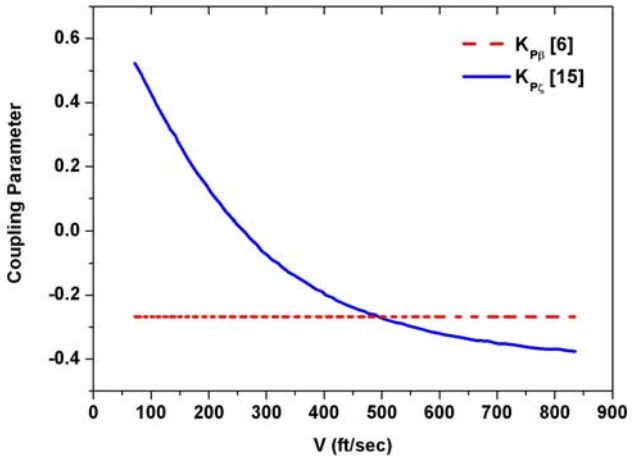

Figure 4 : Effective pitch-flap and pitch-lag coupling parameters

Figure 5 shows the influences of pitch-flap and pitch-lag coupling parameters. If the control system flexibility is not considered, which is $K_{P_\beta} = 0$ and $K_{P_\zeta} = 0$ case, the flutter stability is overestimated over 300 *knots* as compare with baseline in which all coupling parameters are considered. When K_{P_ζ} is neglected, the stability boundary is changed about 180 *knots* from the baseline. In other hand, flutter boundary is slightly increased about 40 *knots* when K_{P_β} is neglected as compare with baseline. Therefore it is clearly that the pitch-lag coupling is the most influence to predict precise flutter stability boundary.

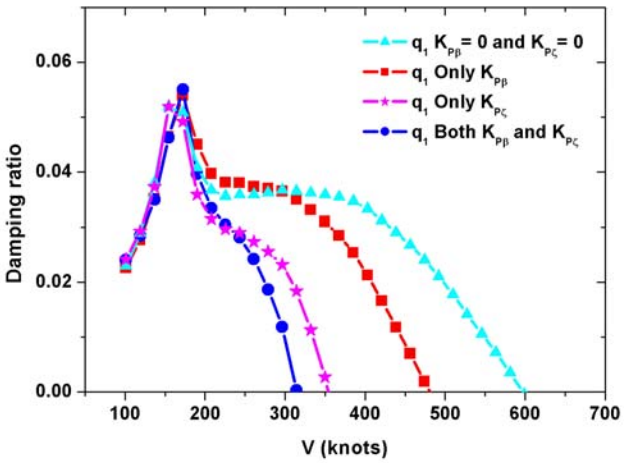

Figure 5 : Comparison results regarding the control system flexibility

3.4 Comparison Results

The present analysis is validated by other numerical results provided in Refs. 6 and 15. The considered analytical model includes the effects of the control system flexibility, wing sweep, wing aerodynamics, and simple aerodynamic coefficient, which only considers lift curve slope, c_{l_α}. The present result shows good agreement with the other existing analyses. The vertical wing mode (q_1) comparison is illustrated in Fig. 5.

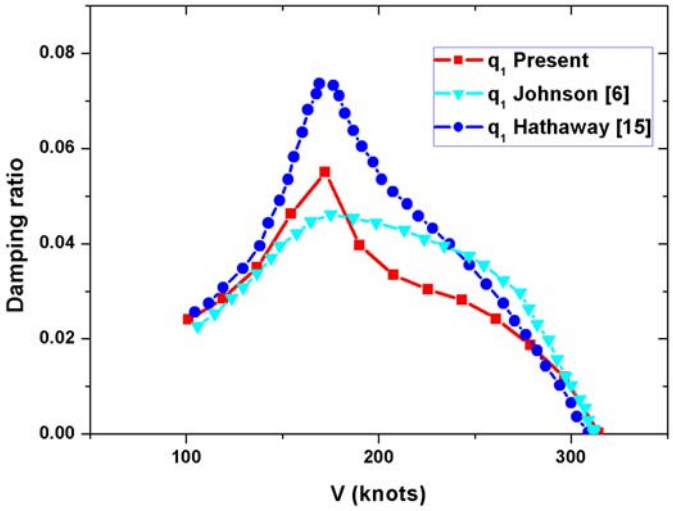

Figure 6 : Damping of the vertical wing mode in terms of the flight speed

All the results show similar stability boundary which is approximately 320 *knots*. The vertical bending (q_1) mode becomes unstable first, and then the chordwise bending (q_2) and torsion (p) mode become unstable. The detailed results will be presented below.

3.5 Results by the Quasi-steady Aerodynamic Models

As mentioned previously, although two different quasi-steady aerodynamic models are used in the present paper, their resulting equations are the same. However the lift formulation has a few different terms. Greenberg's quasi-steady aerodynamic formulation includes two additional terms, while with the normal quasi-steady aerodynamics has only one. Those are $\dot{h}$ and $\dot{\theta}_{ref}$. Here, $\dot{h}$ is velocity of the flapping motion, which is due to $-\delta u_P$ and δu_T components, and $\dot{\theta}_{ref}$ is an angular velocity of the pitch motion with respect to inertial frame. The perturbation term of $\dot{h}$ is described above and $\dot{\theta}_{ref}$ are organized as follow.

$$\delta\theta_{ref} = -K_{p\beta}\beta - K_{p\varsigma}\varsigma + \alpha_y \cos\psi + \alpha_x \sin\psi \tag{8}$$

Figure 7 (a), (b), and (c) illustrate damping of the wing modes, which are vertical bending (q_1), chordwise bending (q_2), and torsion (p) mode, respectively, using the normal and Greenberg's quasi-steady aerodynamic models. They exhibit almost the same stability boundary and variation trend with respect to the flight speed. It is apparent that q_1 mode becomes unstable first at approximately V = 320 *knots* under the both quasi-steady aerodynamic models after that q_2 and p become unstable sequentially.

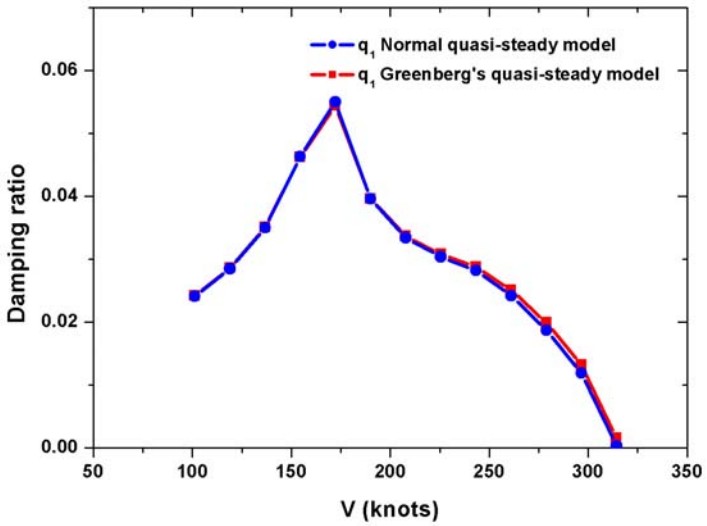

(a) Vertical bending mode with respect to the flight speed

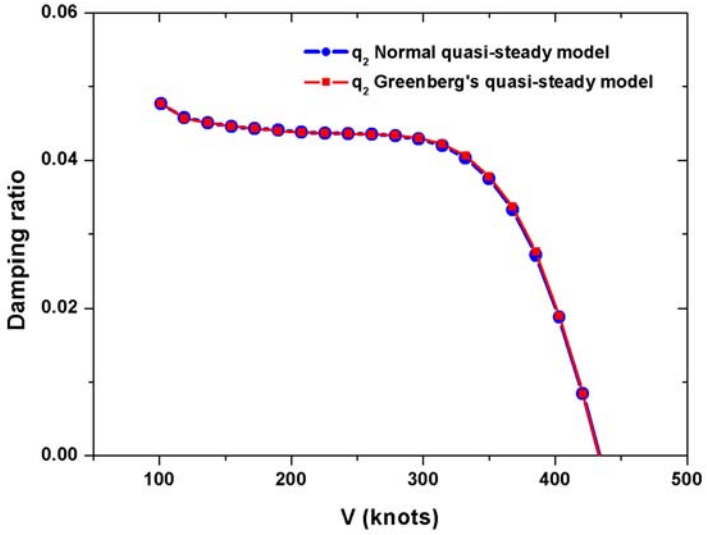

(b) Chordwise bending mode with respect to the flight speed

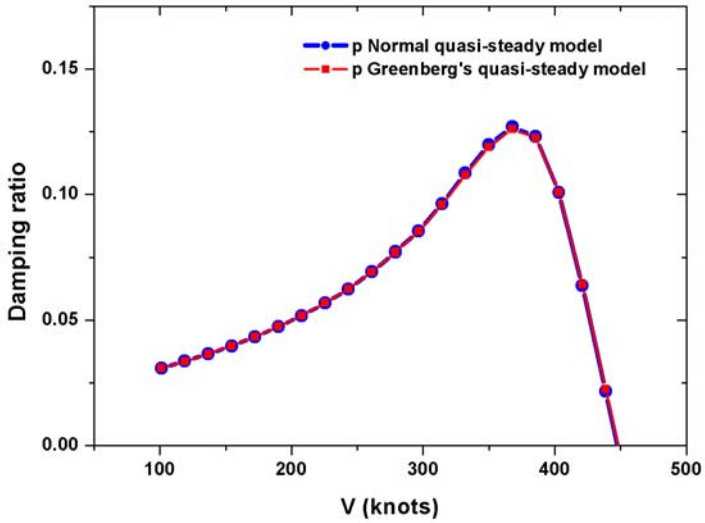

(c) Torsion mode with respect to the flight speed

Figure 7 : Wing mode responses by the normal and Greenberg's quasi-steady aerodynamics

3.6 Results by the Full Unsteady Aerodynamics

Although the quasi-steady aerodynamic models are quite satisfactory for the preliminary analysis, those simple aerodynamic models still have weakness to describe a realistic aerodynamic environment occurring in a tiltrotor aircraft. In this section, numerical investigation is conducted using Greenberg's two-dimensional unsteady aerodynamics. The formulations are derived in time domain by using Jones' approximation. One of the important features of using the full unsteady aerodynamic model in time domain is the transformation of the lift deficiency function, $C(k)$. The augmented state variables are obtained during the transformation. More detailed description and formulations are presented in Refs. 19 and 22.

Figure 8(a) shows the damping of the wing modes in terms of the flight speed. The stability boundary is observed to be approximately 380 *knots*. Here the vertical wing mode (q_1) becomes unstable first among the considered modes. Furthermore q_2 and p modes become consecutively unstable. Figure 8(b) illustrates the comparison results of q_1 mode using three different aerodynamic models. The critical flight speed is predicted to be the highest under the full unsteady aerodynamics as compared with those based on the quasi-steady aerodynamic models. The whirl flutter stability is overestimated by the full unsteady aerodynamic model, by approximately 17% as compared with the result from the quasi-steady aerodynamic models.

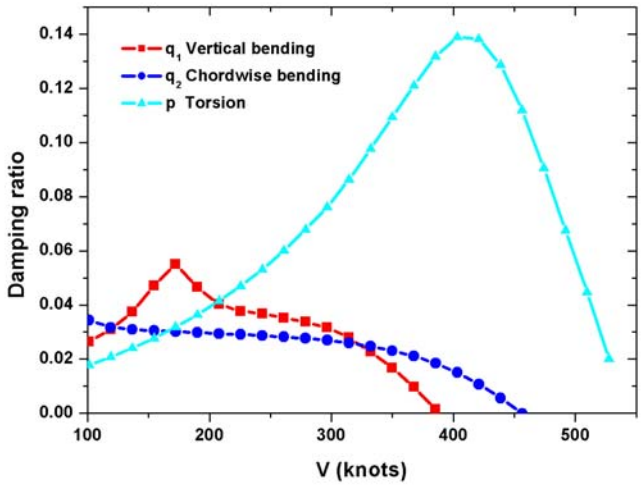

(a) Damping of the wing modes by the full unsteady aerodynamics

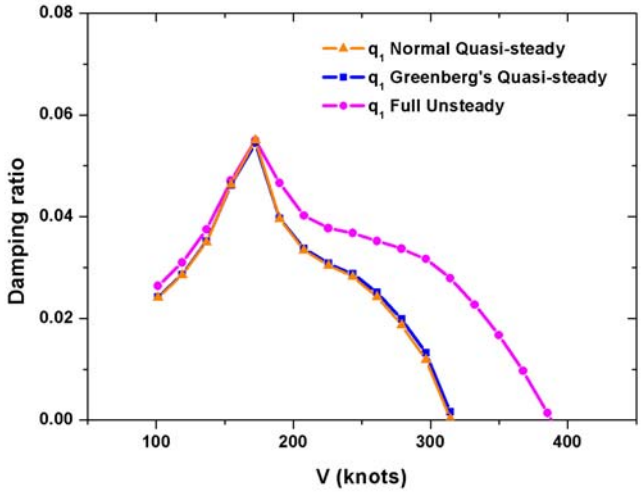

(b) Damping of the wing vertical mode by the three aerodynamic models

Figure 8 : Wing mode results

3.7 Time Domain Result

Time domain results are obtained using the normal quasi-steady aerodynamic model by Runge-Kutta method. The cyclic lag impulse input is used to excite the wing vertical (q_1), chordwise bending (q_2) and torsion (p) modes response, while artificially varying aircraft speed from 285 to 325 knots. In order to vary the flight speed, collective pitch needs to be adjusted. However, in the present numerical examination, the aircraft speed is increased in an arbitrary fashion. Figure 9 shows the results of the wing modes in time domain. It is shown that the aircraft remains stable until

V = 315 *knots*. However, the aircraft becomes unstable when its flight speed is higher than 315 *knots*.

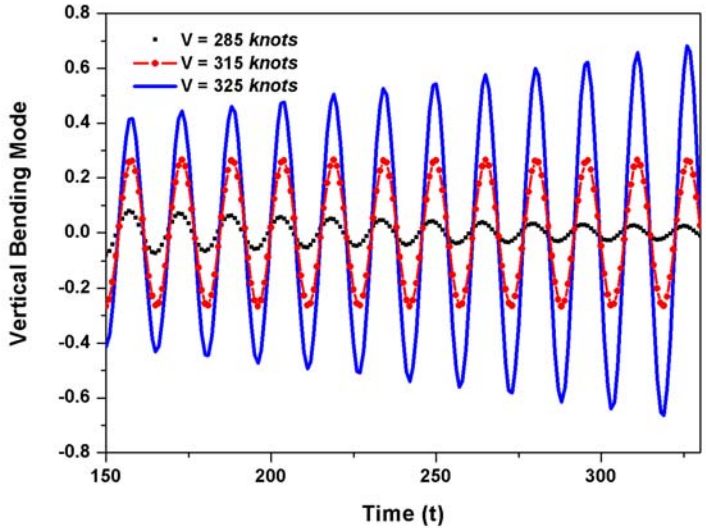

(a) Vertical bending mode in terms of time

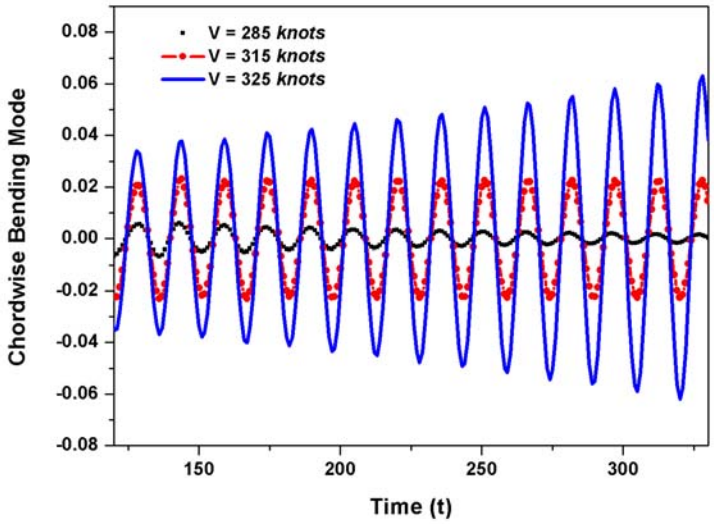

(b) Chordwise bending mode in terms of time

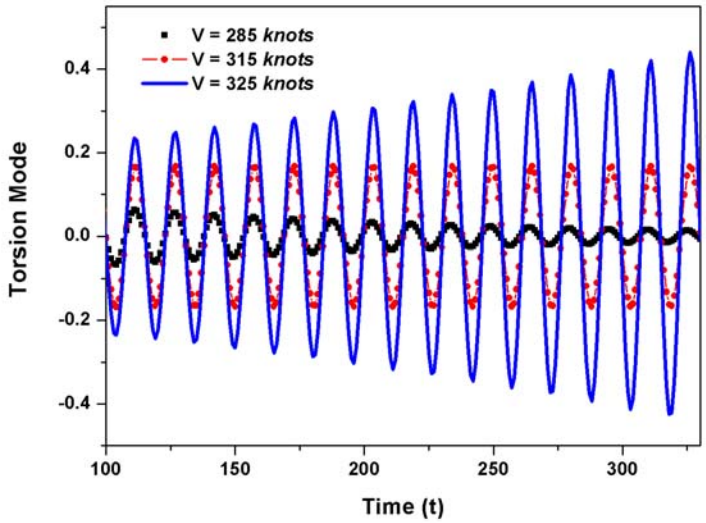

(c) Torsion mode in terms of time

Figure 9 : Time domain analysis results by normal quasi-steady aerodynamic model

4. CONCLUSIONS

Aeroelastic stability analysis is conducted using several structural and aerodynamic features in time and frequency domain. The swept wing and control system flexibility are considered to contrive more complete analytical model. The influence of wing sweep is analyzed by comparing damping ratio of the wing bending mode with and without wing sweep. The damping of the swept wing is smaller than that the straight wing. The stability boundary discrepancy between the swept and straight wing is significant, and therefore the present analytical model includes wing sweep effect.

The wing aerodynamic analysis is performed by using the normal quasi-steady aerodynamic model. Two-dimensional strip theory is used to analyze the wing aerodynamics because of an assumed high aspect ratio. The resulting stability boundary is generally increased when it is compare with that without the wing aerodynamics. It is because the aerodynamic damping effect is generally significant. There is approximately 70 *knots* discrepancy between the results with and without the wing aerodynamics.

The control system flexibility is considered using pitch-flap and pitch-lag coupling parameters. Those coupling parameters are related with blade flexibility as well. The considering control system flexibility is primary influence to predict precise flutter stability boundary. The predicted flutter speed discrepancy is approximately 300 *knots* between with and without control system flexibility.

Finally an analytical model is developed to predict the stability boundary using three different rotor aerodynamic models. The comparison regarding the normal quasi-steady aerodynamics shows a good agreement with the other existing analytical results. Although Greenberg's quasi-steady aerodynamic model predicts a little bit higher flutter speed than the normal quasi-steady aerodynamics, the difference is insignificant. However the flutter boundary with the full unsteady aerodynamic model is approximately 17% overestimated as compare with those from the other two quasi-steady aerodynamics.

At the last stage, time domain analysis is conducted using the normal quasi-steady aerodynamic model. The cyclic lag impulse input is applied to excite the wing modes. And the result shows similar flutter boundary with that obtained from frequency domain analysis.

ACKNOWLEGEMENTS

This work was supported by the Korea Science and Engineering Foundation (KOSEF) grant funded by the Korea Government (MOST) (F01-2007-000-10077-0).

REFERENCES

1. Hall, Jr., W. E., "Prop-Rotor Stability at High Advance Ratios," Journal of the American Helicopter Society, Vol. 11, (2), April 1966.

2. Kvaternik, R. G., and Kohn, J. S., "An Experimental and Analytical Investigation of Proprotor Whirl Flutter," NASA Technical Paper-1047, Dec, 1977.

3. Young, M. I., and Lytwyn, R. T., "The Influence of Blade Flapping Restraint on the Dynamic Stability of Low Disk Loading Propeller-Rotors," Journal of the American Helicopter Society, Vol. 12, (4), Oct. 1967, pp. 38-54.

4. Johnson, W., "Dynamics of Tilting Proprotor Aircraft in Cruise Flight," NASA Technical Note D-7677, May, 1974.

5. Johnson, W., "Analytical model for Tilting Proprotor Aircraft Dynamics Including Blade Torsion and Coupled Bending Modes, and Conversion Mode Operation," NASA TM X-62,369, August, 1974.

6. Johnson, W., "Analytical Modeling Requirements for Tilting Proprotor Aircraft Dynamics," NASA TN D-8013, July, 1975.

7. Nixon, M. W., Kvaternik, R. G., and Settle, T. B., "Tiltrotor Vibration Reduction Through Higher Harmonic Control," American Helicopter Society 53rd Annual Forum, Virginia Beach, Virginia, April 29-May 1, 1977.

8. Kvaternik, R. G., Piatak, D. J., Nixon, M. W., Langston, C. W., Sigleton, J. D., Bennett, R. L., and Brown, R. K., "An Experimental Evaluation of Generalized Predictive Control for Tiltrotor Aeroelastic Stability Augmentation in Airplane Mode of Flight," American Helicopter Society 57th Annual Forum, Washington, DC, May 9-11, 2001.

9. Singh, R. and Gandhi, F., "Wing Flaperon and Swashplate Control for Whirl Flutter Stability Augmentation of a Soft-inplane Tiltrotor," The 31st European Rotorcraft Forum, Florence, Italy, Sept. 13-15, 2005.

10. McVeigh, "The V-22 Tiltrotor Large Scale Rotor Performance/Wing Download Test and Comparison with Theory," 11th European Rotorcraft Forum, London, UK, September, 1985.

11. Felker, F. F. and Light, J. S., "Rotor/Wing Aerodynamic Interactions in Hover," 42nd Annual Forum of the American Helicopter Society, Jun, 1986.

12. McVeigh, M. A., Grauer, W. K., and Paisley, D. L., "Rotor/Airframe Interactions on Tiltrotor Aircrafts," 44th Annual Forum of the American Helicopter Society, Jun, 1988.

13. Felker, F. F., "A Review of Tiltrotor Download Research," 14th European Rotorcraft Forum, September, 1988.

14. Cuzieux, F. and Desopper, A., "Lifting Line Approach for the Modeling of a Tilt-Rotor Wing in HOST: Application to the ERICA Concept," 31st European Rotorcraft Forum, Florence, September 13-15, 2005.

15. Hathaway, E. L., "Active and Passive Techniques for Tiltrotor Aeroelastic Stability Augmentation," Ph.D. Thesis, The Graduate School College of Engineering, The Pennsylvania State University, August, 2005.

16. Bisplinghoff, R. L., Ashley, H., and Halfman, R. L., *Aeroelasticity*, Dover, New York, 1996, Chaps. 6.
17. Greenberg, J. M., "Airfoil in Sinusoidal Motion in Pulsating Stream," NASA TN 1326, 1947.
18. Cesnik, C. E. S., 16.242 Aeroelasticity, Lecture Note, Department of Aeronautics and Astronautics, Massachusetts Institute of Technology, Cambridge, Massachusetts, February 1998.
19. Kim, T. and Shin, S. J., "Advanced Analysis on Tiltrotor Aircraft Flutter Stability, Including Unsteady Aerodynamics," AIAA journal, Vol. 45, No. 4, April 2008.
20. Jones, R. T., "The Unsteady Lift of a Wing of Finite Aspect Ratio," NACA Report 681, 1940.
21. Jones, R. T., "Operational Treatment of the Nonuniform Lift Theory to Airplane Dynamics," NACA TN 667, 1938.
22. Friedmann, P. P. and Robinson, L. H., "Influence of Unsteady Aerodynamics on Rotor Blade Aeroelastic Stability and Response," AIAA Journal, Vol. 28, No. 10, December 1990, pp. 1806-1812.
23. Johnson, W., *Helicopter Theory*, Dover Publications, Inc., New York, 1994.